Available online at www.sciencedirect.com
ScienceDirect
Polymer 48 (2007) 2056–2063
polymer
www.elsevier.com/locate/polymer

Effect of electrical field on polypeptide phase behavior involving a conformationally coupled anisotropic–isotropic transition

Tao Chen, Shaoliang Lin, Jiaping Lin*, Liangshun Zhang

Key Laboratory for Ultrafine Materials of Ministry of Education, School of Materials Science and Engineering, East China University of Science and Technology, 130 Meilong Road, Shanghai 200237, PR China

Received 28 July 2006; received in revised form 31 January 2007; accepted 2 February 2007
Available online 7 February 2007

Abstract

Effect of external electrical field on phase equilibrium was reported for poly(γ-benzyl L-glutamate) (PBLG) in a mixed solvent containing denaturant acid where a helix–coil transition coupled anisotropic–isotropic transition exists. The experimental results revealed that the anisotropic phase and helix conformation can be stabilized when an external electrical field is applied. In the presence of electrical field, the anisotropic–isotropic phase boundary shifts to lower polymer concentrations and the helix–coil induced anisotropic–isotropic transition becomes stable in the denaturant acid. The lattice model derived in our previous work was further generalized by implementing a free energy term contributed from external orientational field of dipole type. The calculated phase diagrams have been compared with those experimentally observed. A good qualitative agreement has been achieved.

Keywords: Helix–coil transition; Electrical field; Liquid crystalline polymer

1. Introduction

Helix–coil conformational transition of polypeptide has been extensively studied as a simple model of a cooperative conformational variation in biological macromolecule [1–3]. Poly(γ-benzyl L-glutamate) (PBLG) is a well-known polypeptide that can exhibit α-helix or coil conformation, depending on temperature and solvent. Above a critical polymer concentration in a helicogenic solvent, such as dichloroethane (DCE), PBLG forms lyotropic liquid crystal where PBLG adopts α-helix conformation. As sufficient organic denaturant solvent, such as dichloroacetic acid (DCA), is added, the above solution undergoes an acid-induced anisotropic–isotropic phase transition caused by helix–coil conformational transition [4,5]. Such a kind of conformational variation coupled phase transition was also observed by cooling down the above solution [4–7]. For example, cooling down PBLG/DCE/DCA solution, the denaturant solvent attacks the hydrogen bond involved in the helical conformation and converts the α-helix into a random coil. The random coil form is predominant at lower temperature where acid molecules are firmly attached to amide linkages. Since the randomly coiled polymer chains are geometrically inconsistent with the long-range orientational order of the liquid crystal, an anisotropic–isotropic transition could be observed at lower temperature.

Since the electrical dipole moment value of a PBLG residue is about 3.5 Debye along its axis [8], the helical rod-like PBLG molecule has a considerable large permanent dipole moment. Such a large dipole moment has its positive pole at the amino end and the negative pole at the carboxy end [9]. Application of an external electrical field is expected to align the rod-like molecules in the direction of electrical field [10] and give a marked effect on either the phase behavior of PBLG liquid crystalline solution or the conformation of PBLG molecules. Some experimental reports regarding the effect of external electrical field on the polypeptide phase equilibrium are available in the literature [11–14]. For example, Toyoshima et al. reported an experimental result of the

* Corresponding author. Tel.: +86 21 64253370; fax: +86 21 64253539.
E-mail address: jplinlab@online.sh.cn (J. Lin).

0032-3861/$ - see front matter © 2007 Elsevier Ltd. All rights reserved.
doi:10.1016/j.polymer.2007.02.001

effect of external electrical field on the high-temperature phase transition between liquid crystalline and isotropic phases in PBLG/1,4-dioxane solution [15]. The existence of electrical field stabilizes the liquid crystalline phase and shifts the anisotropic–isotropic phase transition temperature upward.

In addition to the experimental investigation, theoretical considerations have also been carried out to predict the effect of external field on phase equilibrium of rod-like molecules. Extending Flory's theory of phase equilibrium of rod-like molecules by implanting an additional energy term, Marrucci and Ciferri have first investigated the effect of the external orientational field on the isotropic–anisotropic phase transition [16]. They concluded that the introduction of an external orientational field narrows the biphasic region and shifts the isotropic–anisotropic transition concentration to a lower value. Shibaev et al. have studied the influence of the external orientational field on phase equilibrium of a thermotropic liquid crystalline polymer containing stiff and flexible fragments [17]. They introduced an exact orientational distribution function proposed by Flory and Ronca in the lattice theory. The results showed that the introduction of an external field could stiffen the flexible polymer chain and lead to a stabilized liquid crystalline phase. Sukigara et al. reported the influence of external electrical field on the isotropic–anisotropic phase transition in rod-like polymer solutions by applying the lattice model [18]. The theoretical phase diagram showed that the application of an external electrical field results in a narrower phase transition region and a lower critical concentration for liquid crystal formation. Erman et al. combined the equilibrium lattice model [19] with a lattice flow model [20] to analyze the phase behaviors of block copolymers consisting of rigid blocks and flexible chains in an extensional flow field [21]. They found the biphasic region shifts to lower concentrations with increasing the intensity of the flow field. The orientation degree of rod-like components increases sharply in the presence of the extensional flow field.

However, all these theoretical considerations focus on the rod-like molecules without chain conformational change, and the contribution of the molecular conformational variation has been neglected. Actually, the molecular conformational variation plays an important role in phase transition of polypeptide liquid crystalline solution. Recently, a detailed theoretical study on the effect of the external orientational field on the phase behavior of a binary system involving a conformationally variable polypeptide has been performed by Lin et al. [22]. An energy term related to a quadrupole field was introduced into the lattice model. The calculation results showed that the isotropic–anisotropic phase transition induced by an external orientational field is possible for the polypeptide even with very high chain flexibility as long as the coil–helix chain conformational change is allowed. The external orientational field promotes the combined action of the coil–helix transition and liquid crystal formation. However, the effect of molecular dipole moment of the polypeptide has not been considered in this theoretical model.

So far, either the experimental evidences or the theoretical studies for the effect of external orientational field on phase behavior and molecular conformation of polypeptide are limited. To the best of our knowledge, no literature has been reported for the electrical field effect on the conformationally coupled phase transition of polypeptide liquid crystalline solution. The purpose of present work is to investigate the effect of external electrical field on the phase behaviors, especially the conformationally coupled anisotropic–isotropic phase transition, of PBLG liquid crystalline solutions, i.e. PBLG/chloroform ($CHCl_3$)/trifluoroacetic acid (TFA) solutions. The influences of the external field intensity, polymer concentration and the acid content were studied. To predict the effect of external field on the phase behaviors involving a conformationally coupled anisotropic–isotropic transition, the lattice theory derived in our previous work was further generalize by introducing an energy term contributed from external field of dipole type. Both experimental and theoretical results show that the presence of external electrical field stabilizes the anisotropic phase and helix conformation. As an external electrical field is applied, the isotropic–anisotropic phase boundary shifts to lower polymer concentrations and the helix–coil induced anisotropic to isotropic transition becomes stable in denaturant acid. Qualitatively, the theoretical phase diagrams are in good agreement with the experimental results.

2. Experimental

PBLG samples were synthesized by the *N*-carboxyanhydride method in 1,4-dioxane at room temperature for 72 h with triethylamine as initiator, and subsequently precipitated in a large volume of anhydrous ethanol. The obtained PBLG was purified twice by repeated precipitation from a chloroform solution into a large volume of anhydrous methanol. The viscosity-average molecular weight determined in DCA at 25 °C gives values of 50 000 and 204 000, respectively [23]. Triethylamine and 1,4-dioxane are of analytic grade and dried over sodium and distilled to remove water before use. Tetrachloroethane (TCE), $CHCl_3$, TFA and all other solvents are of analytic grade and used as received.

PBLG solutions were prepared by dissolving measured amount PBLG in a given volume solvent. For PBLG/$CHCl_3$/TFA solutions, $CHCl_3$ and TFA were mixed first with various TFA contents. The polypeptide volume fraction, v_p, was estimated from the density (1.27 g/cm^3) of PBLG. After being homogenized at 25 °C for 24 h, a certain amount of PBLG solution was sealed in a capillary glass tube and stabilized for 2 h before use.

In the case of studying the effect of the external field on the phase transition, a direct current electrical field was applied. The electrical field direction is perpendicular to the axis of the capillary tube. Taking account of the dielectric effect of the air and the glass between the electrodes and PBLG solution, the actual electrical field intensity applied on PBLG solution has been corrected according to Gauss theorem [24]. Some simplifications have been made in correction: the capillary tube wall was simplified as two glass plates to neglect the curvature of the tube wall; the dielectric constants of air, glass and PBLG solution would not change with the variation of

temperature. Thus, the actual electrical field intensity applied on PBLG solution can be given as

$$E = U/\varepsilon_s\left(d_1 + 2d_2/\varepsilon_g + d_3/\varepsilon_s\right) \quad (1)$$

where U is the voltage between the electrodes, d_1 is the total distance between tube outside and electrode board, d_2 is the thickness of the tube wall, d_3 is the inner diameter of tube, ε_g is the dielectric constant of glass with value of 5.60 [24], ε_s is the dielectric constant of PBLG solution, and which can be calculated using equation $\varepsilon_s = \sum_i v_i\varepsilon_i$ where v_i and ε_i are the volume fraction and dielectric constant for the respective components [25]. The dielectric constants of $CHCl_3$, TFA and TCE are 4.90, 8.55 and 5.82, respectively [26]. The dielectric constant of PBLG is reported to be 3.8 [27]. Since the effect of the variation of polymer and solvent concentrations on ε_s is very small in present work (within 2.7%), this effect is neglected for simplicity. Under such a condition, the calculated ε_s for PBLG solutions is 5.6. The field intensities mentioned in this work are all the corrected values.

The phase transition observations were carried out using a Leitz-Ortholux II polarizing microscope. The phase transition temperatures of PBLG solutions were detected by the polarized microscope during heating and cooling of the solutions on a Mettler FP82HT hot stage with a programmable temperature controller. Liquid nitrogen was used to cool down the solution. The heating rate and cooling rate are 1.0 °C min^{-1}, respectively.

3. Experimental results

Fig. 1 shows dependence of phase transition temperatures of PBLG solutions on the intensity of the applied external electrical field. Illustrated in Fig. 1(a) is the result obtained for PBLG/$CHCl_3$/TFA system. In the absence of the external field, PBLG solution shows typical liquid crystal textures within temperature range 60–100 °C. As temperature goes down, isotropic spherulites begin to appear and PBLG solution enters the biphasic phase. With further decreasing temperature, the complete extinction of the anisotropic phase occurs at −10 °C. For PBLG/$CHCl_3$/TFA solution, when the temperature is decreased, TFA acid molecules start interrupting the hydrogen bond involved in the helical architecture and a helix–coil transition takes place [6,7,28,29]. Since the random coil polymer chains are geometrically inconsistent with the long-range orientational order of the liquid crystal, an anisotropic to isotropic transition, where highly cooperative helix–coil transition is coupled, occurs [4,5,28,30]. On the other hand, upon heating PBLG liquid crystalline solution, the helical PBLG chain could become flexible due to the thermal energy, giving rise to a high-temperature anisotropic–isotropic transition as shown in Fig. 1(a). When PBLG solutions are subjected to the external electrical field, the anisotropic phase tends to be stabilized. As it can be seen, with increasing strength of the electrical field, the high-temperature anisotropic–isotropic transition temperature increases, while the low-temperature one decreases.

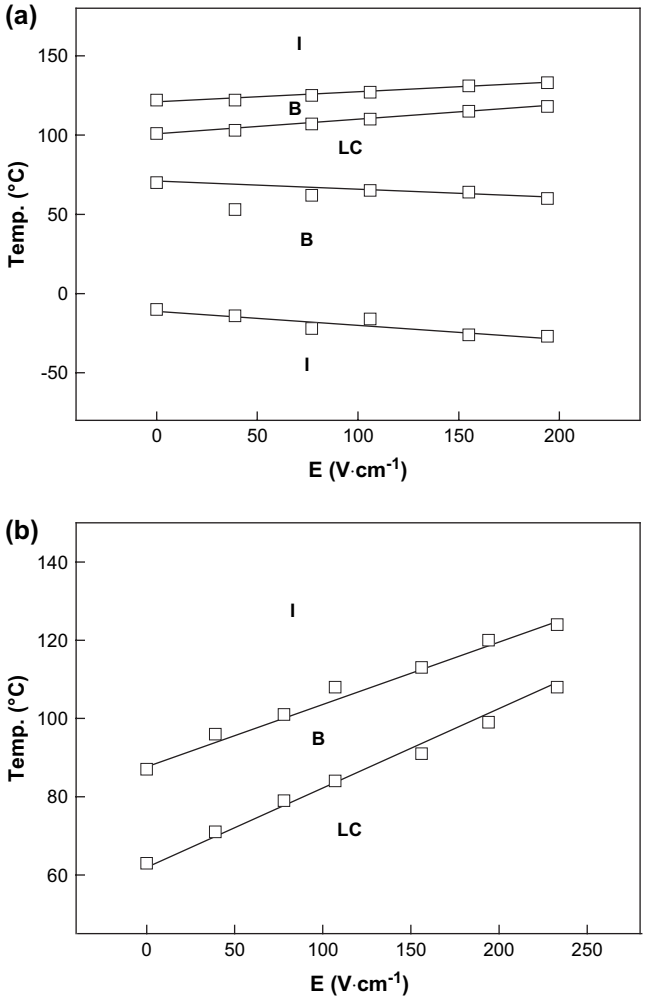

Fig. 1. Experimental phase boundary curves as a function of electrical field intensity for PBLG ($\overline{M}_v = 20.4 \times 10^4$)/$CHCl_3$/TFA solutions with $v_p = 0.204$ and $f_{TFA} = 0.309$ (a) and PBLG ($\overline{M}_v = 5.0 \times 10^4$)/TCE solutions with $v_p = 0.145$ (b). I: isotropic phase; B: biphasic region; LC: liquid crystalline phase.

Observations were also performed for PBLG/TCE systems. The results shown by Fig. 1(b) demonstrate a similar effect on the high-temperature anisotropic to isotropic transition as that of PBLG/$CHCl_3$/TFA system. Such an electrical field dependence of the high-temperature anisotropic–isotropic transition temperature was also reported by Toyoshima et al. for PBLG/1,4-dioxane solution [15]. In addition to the field dependence on the transition temperature, it is noted from Fig. 1 that for both PBLG/$CHCl_3$/TFA and PBLG/TCE systems, the high-temperature anisotropic–isotropic phase boundaries tend to be narrowed as the intensity of the electrical field increases. However, this effect is weak in the low-temperature transition region.

Fig. 2 shows the phase equilibria of PBLG/$CHCl_3$/TFA as a function of polymer volume fraction with and without external electrical field applied. The open squares indicate the observed results for PBLG/$CHCl_3$/TFA solutions without external filed. No anisotropic phase was observed at all temperatures in the range of low polypeptide concentrations. Liquid crystalline

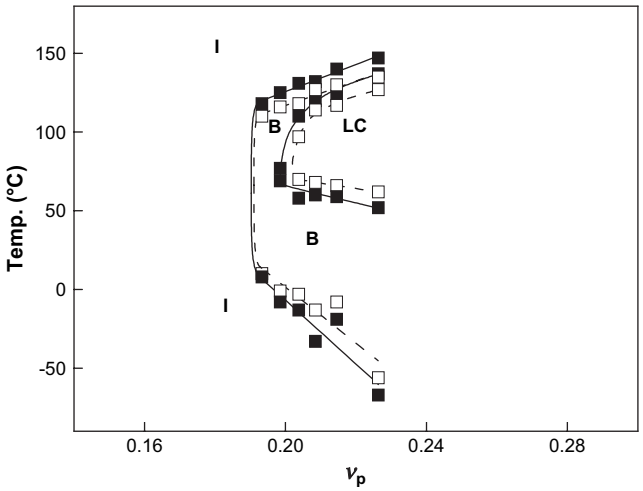

Fig. 2. Experimental phase diagrams for PBLG ($\overline{M}_v = 20.4 \times 10^4$)/$CHCl_3$/TFA solutions with $f_{TFA} = 0.309$ observed in the presence of the electrical field with intensity of $E = 0\ V\ cm^{-1}$ (---□---) and $E = 194\ V\ cm^{-1}$ (—■—). I: isotropic phase; B: biphasic region; LC: liquid crystalline phase.

phase forms as the polymer concentration is increased. The phase diagram presents a similar pattern as those observed in PBLG/DCA/EDC systems [4,5] and PBLG/DCA systems [28]. When an external field with $E = 194\ V\ cm^{-1}$ is applied, the liquid crystalline phase becomes stable in both high- and low-temperature phase boundaries as indicated by the solid squares. The transition temperatures of high- and low-temperature anisotropic–isotropic transitions tend to be higher and lower, respectively. However, the influence of the external electrical field becomes weak in the low-temperature transition range as the polypeptide concentration decreases. It should be noted that the low-temperature anisotropic to isotropic is induced by the intramolecular helix–coil transition. This conformationally coupled phase transition is retarded by the external electrical field. In other words, the anisotropic phase and helix conformation are stabilized by the electrical field.

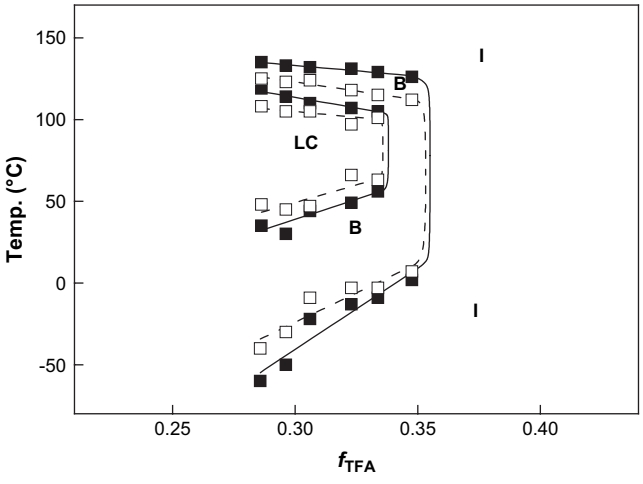

Fig. 3. Experimental phase diagrams for PBLG ($\overline{M}_v = 20.4 \times 10^4$)/$CHCl_3$/TFA solutions with $v_p = 0.204$ observed in the presence of the electrical field with intensity of $E = 0\ V\ cm^{-1}$ (---□---) and $E = 194\ V\ cm^{-1}$ (—■—). I: isotropic phase; B: biphasic region; LC: liquid crystalline phase.

Fig. 3 illustrates the electrical field effect on the phase equilibria of PBLG/$CHCl_3$/TFA as a function of acid content. As it can be seen, the formed anisotropic phase is destabilized along both the high- and low-temperature boundaries when the acid content increases. In the range of a high acid concentration, no anisotropic phase could be observed at all temperatures due to the coil chain conformations being unable to sustain the anisotropic ordering. Such a phenomenon is shown for both PBLG/$CHCl_3$/TFA systems with and without electrical field applied. But in the case of the existence of external electrical field, the liquid crystalline phase is stable in both high and low temperatures. From the phase diagrams, it can be also seen that the influence of the external electrical field turns less pronounced in the low-temperature transition range as the acid content increases.

4. Theoretical consideration

The theoretical model proposed in our previous work [22] mainly focuses on the effect of quadrupole orientational field, which can be caused by uniaxial elongation of polymer solution such as flow of polymer solution, on the conformational variation coupled phase transition; however, the molecular dipole moment has not been considered. In present study, the applied external electrical field is a dipole orientational field, which is different from the quadrupole one. Sukigara et al. have written an expression of energy term related to the external field of dipole type [18]. It is written to be compatible with the present condition as follows

$$E_{ex}/kT = -n_p x^2 \varepsilon_0^2 \left[\frac{\theta p_h^2}{2} \langle \cos^2 \psi_i \rangle + \frac{(1-\theta) p_c^2}{2} \langle \cos^2 \psi_j \rangle \right] \qquad (2)$$

where n_p is the number of the polypeptide with axial ratio x, θ is the helix fraction of the polypeptide and the dimensionless parameter ε_0 defines the intensity of the applied external electrical field, p_h and p_c are the dipole moments of a lattice segment of polypeptide with helix and coil conformation, respectively. In the above equation, the averaging is performed over all angles ψ_i between the rigid helix segment and the orientation axis and over all ψ_j between the links of the flexible coil component and the orientation axis [31].

The mixing free energy expression for a system involving a polypeptide, a randomly coiled polymer, and a solvent has been written out in our previous work [32]. The expression can be readily turned to a binary system consisting of a polypeptide chain and a solvent by setting the concentration of the randomly coiled polymer as zero and written as

$$\begin{aligned} -\ln Z_M = {} & n_s \ln v_s + n_p \ln v_p + x n_p (1 - 1/x) \\ & - n_0 [(1-Q)\ln(1-Q) + Q] + \chi x (n_p n_s / n_0) \\ & - mx n_p [\theta(\beta + \ln s) + \rho \ln(\sigma S_0) \\ & \quad - (1-\theta-\rho)\ln(1-\theta-\rho) - \rho \ln \rho \\ & \quad + (1-\theta)\ln(1-\theta)] \end{aligned} \qquad (3)$$

where n_s is the number of the solvent molecule, v_s and v_p represent the volume fractions of the solvent and polymer,

n_0 equals $n_s + xn_p$, s and σ denotes, respectively, the statistical weight for a unit in the helical state relative to the coil and the weighting factor for initiation of a helical sequence, m represents the number of repeat units (i.e., peptide residues) in the lattice segment, ρ is the fraction of units that mark the beginning of a helical sequence, β is a Lagrangian multiplier, χ is the polymer–solvent interaction parameter, and Q and S_0 are orientation-related quantities that have been defined in Ref. [32].

When the binary system is subjected to an external electrical field, an extra term expressed by Eq. (2) should be included in the lattice scheme. After incorporating Eq. (2), the mixing free energy expression becomes

$$\begin{aligned}-\ln Z_M = {} & n_s \ln v_s + n_p \ln v_p + xn_p(1-1/x) \\ & - n_0[(1-Q)\ln(1-Q)+Q] + \chi x\left(n_p n_s/n_0\right) \\ & - mxn_p[\theta(\beta+\ln s)+\rho\ln(\sigma S_0) \\ & \quad - (1-\theta-\rho)\ln(1-\theta-\rho) \\ & \quad - \rho\ln\rho + (1-\theta)\ln(1-\theta)] \\ & - n_p x^2\varepsilon_0^2\left[\frac{\theta p_h^2}{2}\langle\cos^2\psi_i\rangle + \frac{(1-\theta)p_c^2}{2}\langle\cos^2\psi_j\rangle\right] \end{aligned} \quad (4)$$

In the anisotropic phase, the calculations revealed that the maximum stability occurs at $\theta = 1$. Under such a circumstance, the last term of Eq. (4), which is contributed from the external electrical field, reduces to $-((x^2p_h^2n_p\varepsilon_0^2)/2)\langle\cos^2\psi_i\rangle$. With further substituting the conditions for the anisotropy as specified in Ref. [32], Eq. (4) becomes

$$\begin{aligned}-\ln Z_M = {} & n_s \ln v_s' + n_p \ln v_p' + xn_p(1-1/x) \\ & - n_0[(1-Q)\ln(1-Q)+Q] + \chi x\left(n_p n_s/n_0\right) \\ & - n_p\left[\ln(y/x)^2 + mx\ln s + \ln\sigma\right] - \frac{x^2p_h^2n_p\varepsilon_0^2}{2} \end{aligned} \quad (5)$$

where the prime symbol ($'$) is appended to denote the anisotropic phase.

Since the polypeptide chain takes a fully helix form in the anisotropic phase, the exact lattice treatment according to Flory and Ronca [33] is utilized for the deduction of the disorientation parameter y. The external field also affects the orientational distribution, which makes a further contribution to the reduced free energy. Therefore, f_p adopted by Flory and Ronca is redefined as

$$f_p = \int_0^{\pi/2} \sin^p\psi \exp\left(-\alpha\sin\psi - \frac{x^2p_h^2\varepsilon_0^2}{2}\sin^2\psi\right)d\psi \quad (6)$$

$$\alpha = -(4/\pi)x\ln\left[1 - v_p'(1-y/x)\right] \quad (7)$$

$$y = (4/\pi)x(f_2/f_1) \quad (8)$$

and the quantity Q is given by

$$Q = v_p'\left(1 - \frac{4f_2}{\pi f_1}\right) \quad (9)$$

Chemical potentials of the components in the anisotropic phase can be readily obtained by partially differentiating Eq. (5) with auxiliary Eqs. (6)–(9). The results are shown as

$$\Delta\mu_s' = \ln v_s' + v_p'\left(1-\frac{1}{x}\right) + \chi v_p'^2 - \ln(1-Q) - Q \quad (10)$$

$$\begin{aligned}\Delta\mu_p' = {} & \ln v_p' + xv_p'\left(1-\frac{1}{x}\right) + \chi v_s'^2 - xQ \\ & - \ln f_1 - (mx\ln s + \ln\sigma) - \frac{x^2p_h^2\varepsilon_0^2}{2}\end{aligned} \quad (11)$$

In the state of the isotropy, the orientational order parameter $S = (3\langle\cos^2\psi_i\rangle - 1)/2 = 0$; thus, $\langle\cos^2\psi_i\rangle = 1/3$. The $\langle\cos^2\psi_j\rangle$ term is also equal to 1/3 due to the random orientations [17,28]. Therefore, the last term of Eq. (4) appears to be $-((\theta p_h^2 + (1-\theta)p_c^2)/6)n_p x^2\varepsilon_0^2$. Incorporating this result, together with the conditions obtained for the isotropy according to Ref. [32], into Eq. (4) gives

$$\begin{aligned}-\ln Z_M = {} & n_s \ln v_s + n_p \ln v_p + n_p(x-1) \\ & + \chi x\left(n_p n_s/n_0\right) + mxn_p\ln[1-\rho/(1-\theta)] \\ & - \frac{\theta p_h^2 + (1-\theta)p_c^2}{6} n_p x^2\varepsilon_0^2\end{aligned} \quad (12)$$

Partial differentiation of the above equation yields the reduced chemical potentials of the components in the isotropic phase.

$$\Delta\mu_s = \ln v_s + v_p\left(1-\frac{1}{x}\right) + \chi v_p^2 \quad (13)$$

$$\begin{aligned}\Delta\mu_p = {} & \ln v_p + xv_p\left(1-\frac{1}{x}\right) + \chi v_s^2 + mx\ln[1-\rho/(1-\theta)] \\ & - \frac{\theta p_h^2 + (1-\theta)p_c^2}{6} x^2\varepsilon_0^2\end{aligned} \quad (14)$$

According to Ref. [30], the statistical weight s can be related to a change in Gibbs free energy ΔG_0 for the helix formation

$$s = \exp(-\Delta G_0/RT) = \exp(-\Delta H_0/RT + \Delta S_0/R) \quad (15)$$

where ΔG_0 is broken up into an intrinsic enthalpy and entropy change, ΔH_0 and ΔS_0, respectively. For polypeptides with high molecular weight, the helix fraction θ is given by [5]

$$\theta = 1/2 + (s-1)/2\left[(1-s)^2 + 4\sigma s\right]^{1/2} \quad (16)$$

When a denaturant acid is present, the factor of s should be replaced by [5]

$$s_c = s/(1+Ka) \quad (17)$$

where a is the acid activity proportional to the denaturant acid content and K is the equilibrium constant due to the binding which occurs through hydrogen bonding to exposed amide linkages in the coiled state. K is written in an expression form

$$K = \exp(-\Delta G_c/RT) = \exp(-\Delta H_c/RT + \Delta S_c/R) \quad (18)$$

where $\Delta H_c < 0$ and $\Delta S_c < 0$.

To properly account for the phase behavior, especially the high-temperature anisotropic–isotropic phase transition, the axial ratio x is replaced by a temperature-dependent Kuhn chain axial ratio $x_k = 80\,000/T$ [22]. Furthermore, the parameter χ is related to temperature by $\chi = -A + B/T$ with A and B specified as 1.667 and 352 [5]. The A and B values are adopted to simulate the experimental phase behaviors to the greatest extent in our work [5,22,28,30,32].

The relations governing the phase equilibria of the binary system in the presence of the external electrical field can be obtained by equating Eq. (10) to Eq. (13), Eq. (11) to Eq. (14) with auxiliary relations of Eqs. (6)–(9) and Eqs. (15)–(18). The effects of the external electrical field intensity on phase equilibria are illustrated in Fig. 4 where the field intensity ε_0 is plotted against T. In numerical calculation, m is set as 10 [34], which means each lattice segment contains 10 peptide residues. The electrical dipole moment value of PBLG residue is reported to be 3.5 Debye [8], thus p_h is 35 Debye for a lattice segment of rigid helical PBLG molecule. According to mean square end-to-end distance of free rotation chain and the bond length and bond angle of PBLG residue [35], p_c was calculated to be 2.5 Debye per lattice segment for randomly coiled PBLG segments. ε_0 can be associated with the electrical field intensity in experiment by multiplying a physical unit. According to Ref. [36], the physical unit can be $\tau = (kT/\xi_0 v_{LC})^{1/2}$, where k is the Boltzmann constant, T is the average experimental temperature, ξ_0 is the vacuum permittivity, and v_{LC} is the volume of per polypeptide molecule. Therefore, we can qualitatively compare the theoretical results with experimental results. As it can be seen from Fig. 4, by increasing the value of ε_0, the anisotropic phase becomes stable. The high-temperature anisotropic–isotropic transition temperature increases, while the low-temperature one decreases. Increasing field intensity also narrows the biphasic phase separation region. Within the low-temperature range, the intramolecular helix–coil conformational changes are coupled with the intermolecular anisotropic–isotropic phase transition. This transition is calculated to be retarded by the external electrical field. The theoretical calculation qualitatively reproduced the general feature of the experimental results as shown in Fig. 1, i.e. the high-temperature and low-temperature anisotropic–isotropic transition temperatures become higher and lower, respectively, in the presence of electrical field and the phase boundary tends to be narrowed when the external electric field intensity increases in high temperatures.

The role of the external electrical field was also shown in Fig. 5 where transition temperature is plotted against polymer concentration for $\varepsilon_0 = 0$ and $\varepsilon_0 = 0.0004$. Other parameters used for numerical calculations are listed in the caption. As shown in Fig. 5, the existence of the external electrical field tends to narrow the biphasic phase separation region and shifts the anisotropic–isotropic transition to lower polymer concentrations. Comparison of the calculation results with the phase diagram of Fig. 2 shows that the experimental result agrees well with the theoretical predication.

Illustrated in Fig. 6 is the relationship between the phase equilibria and the acid activity with and without electrical field applied. Liquid crystalline phase is calculated to be stable at lower acid activity, and it transforms into isotropic phase as acid activity increases. This intermolecular transition is induced by the helix–coil transition. When an external electrical field is applied, the anisotropic–isotropic phase boundary shifts to higher acid activity and biphasic region becomes narrower concomitantly. Theoretically calculated phase diagram is in line with the experimental phase diagram in Fig. 3. Both results show that the anisotropic phase becomes stable in high denaturant acid content when an external electrical field is applied.

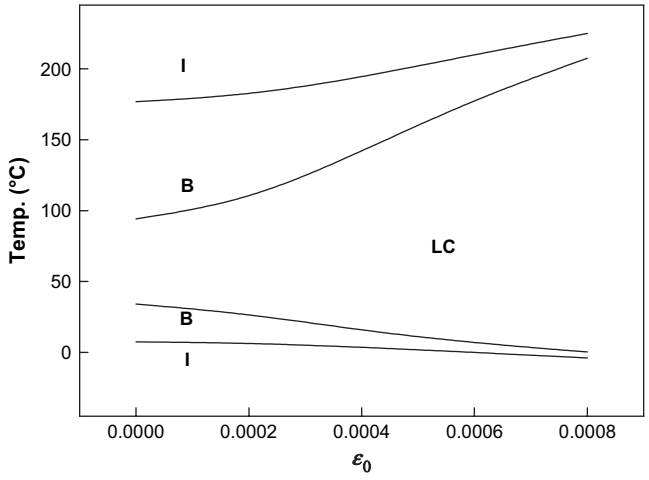

Fig. 4. Calculation results for the phase transition temperatures as a function of the external field at a given polymer concentration of $v_p = 0.20$. Invariant parameters used in the calculations are $\Delta H_0 = -1500.0$ cal mol^{-1}, $\Delta S_0 = -1.2$ cal mol^{-1} K^{-1}, $\Delta H_c = -2000.0$ cal mol^{-1}, $\Delta S_c = -1.0$ cal mol^{-1} K^{-1}, $R = 1.987$ cal mol^{-1} K^{-1}, $a = 0.32$, $m = 10$, $\sigma = 10^{-4}$, $p_h = 35$, $p_c = 2.5$. I: isotropic phase; B: biphasic region; LC: liquid crystalline phase.

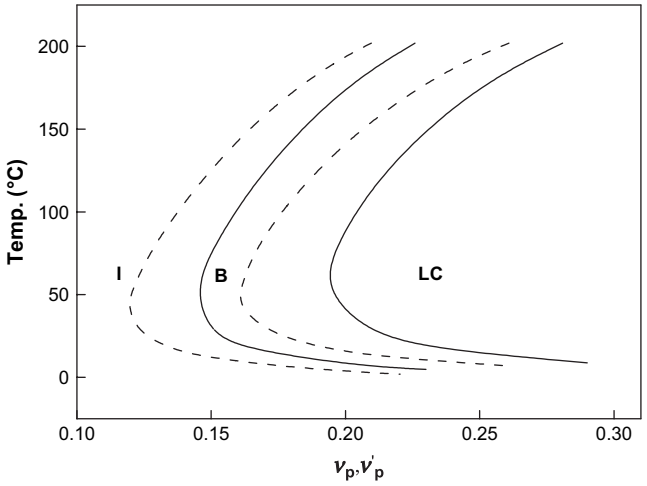

Fig. 5. Anisotropic–isotropic phase equilibria as a function of polymer concentration calculated at $\varepsilon_0 = 0$ (solid line) and $\varepsilon_0 = 0.0004$ (dash line). Other parameters used in the calculations are similar to those in Fig. 4. I: isotropic phase; B: biphasic region; LC: liquid crystalline phase.

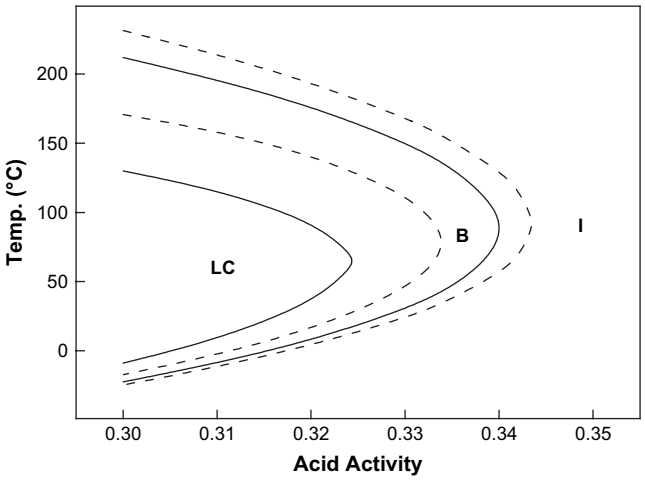

Fig. 6. Anisotropic–isotropic phase equilibria as a function of acid activity calculated at $\varepsilon_0 = 0$ (solid line) and $\varepsilon_0 = 0.0004$ (dash line). Other parameters used in the calculations are similar to those in Fig. 4. I: isotropic phase; B: biphasic region; LC: liquid crystalline phase.

Experimentally, with microscope there had been a difficulty in determining the I/B phase boundary at lower v_p due to very small amount of liquid crystals in form of dim specks in the dark field of vision (Fig. 2). Also, owing to the reasons that very small amount of isotropic drops in the light filed of vision during LC → B transition and very small amount of dim liquid crystal specks in the dark field of vision upon B → I transition, it is difficult to find the LC/B and B/I phase boundaries at higher f_{TFA} (Fig. 3). The sharp boundaries at lower v_p and higher f_{TFA} in Figs. 2 and 3 just schematically represent the phase boundaries. However, the theoretical calculations predicted these boundaries as shown in Figs. 5 and 6.

5. Discussion

Despite some difference between theoretical and experimental results, either experimental or theoretical phase diagrams show that the application of external electrical field stabilizes the liquid crystalline phase and helix conformation of polypeptide. The transition temperatures of high- and low-temperature anisotropic–isotropic transitions tend to be higher and lower, respectively. In the presence of external electrical field, the isotropic–anisotropic phase boundary shifts to lower polymer concentrations. For the solution containing organic acid, the existence of external electric field would stabilize the anisotropic phase and make the anisotropic–isotropic phase boundary to higher acid concentration, i.e. more denaturant acid is needed to induce helix–coil coupled anisotropic–isotropic phase transition.

As indicated in our previous work [5], due to the difficulties in relating some theoretical parameters to the conventional measurements of quantities, a quantitative comparison between the theory and experiments becomes difficult. However, the qualitative agreement between the theory and experiments can still be improved. For example, since the variation of the denaturant acid content is small in the present work, we ignored the dependence of χ on the acid concentration for simplicity. In the experiments, χ could become more negative as the acid activity increase. If this effect is considered, the agreement between the theory and experiments could be improved. Moreover, the comparisons between the theoretical and experimental results (Fig. 4 and Fig. 1(a)) show that the theoretical prediction for low-temperature biphasic range is smaller than that from experimental results, while the high-temperature biphasic range is larger than that from experimental results. Our calculations show that decrease in the statistical weight parameter s of Eq. (3), which is associated with the nature of the helix–coil transition, can broaden the low-temperature anisotropic–isotropic range. On the other hand, the effect of orientation dependent interaction is not considered for simplicity in the present work. As revealed by our previous work [30], the existence of the orientation dependent interaction can narrow the biphasic regions of both high- and low-temperature anisotropic–isotropic transitions. If these two effects are considered in the theory, the agreement between the experiments and theory can be further improved by adjusting the influence imposed by s and orientation dependent interaction.

In spite of its artificiality, the lattice model has been proved successful in the treatments of the polymeric liquid crystal systems [37,38] and has been extended to various systems [19,39–42]. Our series work further extended the lattice model to the treatments of the biopolypeptide systems, such as reentrant transitions in the polypeptides [4,28,30], ternary mixtures involving a polypeptide with and without an external quadrupole orientational field applied [31,32]. In present work, after including the free energy arising from the dipole type external orientational field into the lattice scheme, the lattice theory provides a reasonable insight for the conformational transition coupled phase behaviors of the binary systems containing a polypeptide and a solvent in the presence of the external dipole orientational field.

The conformationally coupled phase transitions stimulated by an external electrical field, which are studied in present work, may find the future utilization in information storage and processing devices [43,44]. For instance, the helix formation is a highly cooperative process along the molecular axis; the information would spread along the polypeptide main chain with a very high speed. Such feature makes the polypeptide qualified for the potential utilization in biological computer [45]. In addition, the conformational transition of proteins plays an important role in biological activities of cells and organism. The external electrical filed was found to change the conformation of proteins and further affect the physiological activities of cells and organism [46,47]. Since the polypeptide has the similar peptide backbone and secondary structures as those of proteins, it provides a useful model to investigate the relationships between the conformations and the properties of proteins. The results of present research of the electrical field effect on polypeptide conformationally coupled phase transition may offer some useful information to understand the structures and properties of proteins [48].

6. Conclusions

In present work, we have investigated the effect of an external electrical field on helix–coil coupled anisotropic–isotropic phase transition of PBLG/$CHCl_3$/TFA solutions by polarizing microscope. To account for the electrical field influence, the lattice model derived in our previous work was further generalized by implementing a free energy term contributed from external orientational field of dipole type. Both experimental and theoretical results revealed that the anisotropic phase where polypeptide adopts α-helix form tends to be stabilized as the intensity of the external electrical field increases. The isotropic–anisotropic phase boundary shifts to lower polymer concentrations and the helix–coil induced anisotropic–isotropic transition becomes stable in denaturant acid as the external electrical field is applied. Qualitatively, the theoretical predictions are in good agreement with the experimental results.

Acknowledgements

This work was supported by the National Natural Science Foundation of China (20574018, 50673026). Supports from Doctoral Foundation of Education Ministry of China (Grant No. 20050251008). Program for New Century Excellent Talents in University in China (NCET-04-0410), and Project of Science and Technology Commission of Shanghai Municipality (05DJ14005) are also appreciated.

References

[1] Engel J, Schawrz G. Angew Chem Int Ed 1970;9:389–400.
[2] Schawrz G, Engel J. Angew Chem Int Ed 1972;11:568–75.
[3] Inomata K, Kasuya M, Sugimoto H, Nakanishi E. Polymer 2005;46:10035–44.
[4] Lin J, Abe A, Furuya H, Okamoto S. Macromolecules 1996;29:2584–9.
[5] Lin J. Polymer 1997;38:4837–41.
[6] Subramanian R, Wittebort RJ, DuPre DB. Mol Cryst Liq Cryst 1983;97:325–36.
[7] Subramanian R, DuPre DB. J Chem Phys 1984;87:4626–9.
[8] Wada A. J Polym Sci 1960;45:145–54.
[9] Branden C, Tooze J. Introduction to protein structure. 2nd ed. New York: Garland Publishing; 1998. p. 16.
[10] Duke RW, DuPre DB. Macromolecules 1974;7:374–6.
[11] Iizuka E. Biochim Biophys Acta 1969;175:457–9.
[12] Iizuka E. Biochim Biophys Acta 1971;243:1–10.
[13] Toth WJ, Tobolsky AV. Polym Lett 1970;8:531–6.
[14] Stamatoff JB. Mol Cryst Liq Cryst 1972;16:137–42.
[15] Toyoshima Y, Minami N, Sukigara M. Mol Cryst Liq Cryst 1976;35:325–35.
[16] Marrucci G, Ciferri A. J Polym Sci Polym Lett Ed 1977;15:643–8.
[17] Vasilenko SV, Khokhlov AR, Shibaev VP. Macromolecules 1984;17:2275–9.
[18] Aikawa Y, Minami N, Sukigara M. Mol Cryst Liq Cryst 1981;70:115–27.
[19] Matheson RR, Flory PJ. Macromolecules 1981;14:954–60.
[20] Bahar I, Erman B. J Polym Sci Part B Polym Phys 1986;24:1361–71.
[21] Curgul S, Erman B. Polymer 2005;46:275–81.
[22] Lin J, Zhou H, Zhou D. Polymer 2001;42:549–54.
[23] Doty P, Bradbury JH, Holtzer AH. J Am Chem Soc 1956;78:947–54.
[24] Wolfson R, Pasachoff JM. Physics for scientists and engineers. 3rd ed. New York: Addison Wesley; 1999 [chapters 24, 26].
[25] Jouyban A, Soltanpour S, Chan HK. Int J Pharm 2004;353–60.
[26] Wypych G. Handbook of solvents. Beijing: Chemical Industry Press; 1997.
[27] Nakiri T, Imoto K, Ishizuka M, Okamoto S, Date M, Uematsu Y, et al. Jpn J Appl Phys 2004;43:6769–74.
[28] Lin J, Liu N, Chen J, Zhou D. Polymer 2000;41:6189–94.
[29] Suzuki Y, Inoue Y, Chujo R. Biopolymers 1975;14:1223–30.
[30] Lin J. Polymer 1998;39:5495–500.
[31] Lin J, Lin S, Chen T, Tian X. Macromolecules 2004;37:5461–7.
[32] Lin J, Lin S, Liu P, Hiejima T, Furuya H, Abe A. Macromolecules 2003;36:6267–72.
[33] Flory PJ, Ronca G. Mol Cryst Liq Cryst 1979;54:289–310.
[34] Flory PJ, Matheson RR. J Phys Chem 1984;88:6606–12.
[35] Abe A, Yamazaki T. Macromolecules 1989;22:2138–45.
[36] Lin CY, Schick M. Macromolecules 2005;38:5766–73.
[37] Flory PJ. Adv Polym Sci 1984;59:1–36.
[38] Abe A, Ballauff M. In: Ciferri A, editor. Liquid crystallinity in polymers. New York: VCH; 1991. p. 131–67.
[39] Abe A, Flory PJ. Macromolecules 1978;11:1122–6.
[40] Frost RS, Flory PJ. Macromolecules 1978;11:1134–8.
[41] Flory PJ. Macromolecules 1978;11:1138–41.
[42] Flory PJ. Macromolecules 1978;11:1141–4.
[43] Shibaev VP, Plate NA. Adv Polym Sci 1984;60/61:173–252.
[44] Mittal KL. Polymers in information storage technology. New York: Plenum Press; 1989.
[45] Hunter L. Artificial intelligence and molecular biology. Menlo Park: AAAI Press; 1993 [chapter 1].
[46] Budi A, Legge FS, Treutlein H, Yarovsky I. J Phys Chem B 2005;109:22641–8.
[47] Yeom HY, Zhang QH, Dunne CP. Food Chem 1999;67:53–9.
[48] Neumann E. Prog Biophys Mol Biol 1986;47:197–231.